Parasitol Res (2016) 115:1085–1096
DOI 10.1007/s00436-015-4838-8

ORIGINAL PAPER

Hydrothermal synthesis of titanium dioxide nanoparticles: mosquitocidal potential and anticancer activity on human breast cancer cells (MCF-7)

Kadarkarai Murugan[1] · Devakumar Dinesh[1] · Krishnamoorthy Kavithaa[2] · Manickam Paulpandi[1] · Thondhi Ponraj[1] · Mohamad Saleh Alsalhi[3] · Sandhanasamy Devanesan[3] · Jayapal Subramaniam[1] · Rajapandian Rajaganesh[1] · Hui Wei[4] · Suresh Kumar[5] · Marcello Nicoletti[6] · Giovanni Benelli[7]

Received: 22 October 2015 / Accepted: 17 November 2015 / Published online: 1 December 2015

Abstract Mosquito vectors (Diptera: Culicidae) are responsible for transmission of serious diseases worldwide. Mosquito control is being enhanced in many areas, but there are significant challenges, including increasing resistance to insecticides and lack of alternative, cost-effective, and eco-friendly products. To deal with these crucial issues, recent emphasis has been placed on plant materials with mosquitocidal properties. Furthermore, cancers figure among the leading causes of morbidity and mortality worldwide, with approximately 14 million new cases and 8.2 million cancer-related deaths in 2012. It is expected that annual cancer cases will rise from 14 million in 2012 to 22 million within the next two decades. Nanotechnology is a promising field of research and is expected to give major innovation impulses in a variety of industrial sectors. In this study, we synthesized titanium dioxide (TiO_2) nanoparticles using the hydrothermal method. Nanoparticles were subjected to different analysis including UV–Vis spectrophotometry, Fourier transform infrared spectroscopy (FTIR), X-ray diffraction (XRD), field emission scanning electron microscopy (FESEM), zeta potential, and energy-dispersive spectrometric (EDX). The synthesized TiO_2 nanoparticles exhibited dose-dependent cytotoxicity against human breast cancer cells (MCF-7) and normal breast epithelial cells (HBL-100). After 24-h incubation, the inhibitory concentrations (IC_{50}) were found to be 60 and 80 μg/mL on MCF-7 and normal HBL-100 cells, respectively. Induction of apoptosis was evidenced by Acridine Orange (AO)/ethidium bromide (EtBr) and 4′,6-diamidino-2-phenylindole dihydrochloride (DAPI) staining. In larvicidal and pupicidal experiments conducted against the primary dengue mosquito *Aedes aegypti*, LC_{50} values of nanoparticles were 4.02 ppm (larva I), 4.962 ppm (larva II), 5.671 ppm (larva III), 6.485 ppm (larva IV), and 7.527 ppm (pupa). Overall, our results suggested that TiO_2 nanoparticles may be considered as a safe tool to build newer and safer mosquitocides and chemotherapeutic agents with little systemic toxicity.

Keywords Apoptosis · Antibacterial activity · Chemotherapy · Cytotoxicity · DAPI · MCF-7 cells · TiO_2 · Western blot

✉ Giovanni Benelli
g.benelli@sssup.it; benelli.giovanni@gmail.com

[1] Department of Zoology, School of Life Sciences, Bharathiar University, Coimbatore, Tamil Nadu 641046, India

[2] Department of Biochemistry, Biotechnology and Bioinformatics, Avinashilingam Institute for Home Science and Higher Education for Women University, Coimbatore, Tamil Nadu 641043, India

[3] Department of Physics and Astronomy, Research Chair in Laser Diagnosis of Cancer, King Saud University, Riyadh, Kingdom of Saudi Arabia

[4] Institute of Plant Protection, Fujian Academy of Agricultural Sciences, Fuzhou 350013, Fujian, People's Republic of China

[5] Department of Medical Microbiology and Parasitology, Faculty of Medicine and Health Sciences, Universiti Putra Malaysia, Serdang, Malaysia

[6] Department of Environmental Biology, Sapienza University of Rome, Piazzale Aldo Moro 5, 00185 Rome, Italy

[7] Insect Behaviour Group, Department of Agriculture, Food and Environment, University of Pisa, via del Borghetto 80, 56124 Pisa, Italy

Introduction

Mosquito vectors (Diptera: Culicidae) are responsible for transmission of serious diseases worldwide (Benelli 2015). Only India reports 1.48 million malaria cases and about 173 deaths: 1.4 million suspected and 11,985 confirmed chikungunya cases; 5,000 Japanese encephalitis cases and approximately 1,000 deaths; and 383 dengue cases and 6 deaths during 2006 and 2007 (Kovendan et al. 2012). *Aedes aegypti* is a primary vector of dengue fever in tropical and sub-tropical regions around the world (WHO 2012). Recently, dengue transmission has strongly increased in urban and semi-urban areas, becoming a major international public health concern. Over 2.5 billion people are now at risk from dengue. The World Health Organization estimates that there may be 50–100 millions of dengue infections worldwide every year (WHO 2012). Culicidae control is being enhanced in many areas, but there are significant challenges, including an increasing mosquito resistance to insecticides and a lack of alternative, cost-effective, and eco-friendly insecticides (Benelli 2015). To deal with these crucial challenges, recent emphasis has been placed on plant materials with mosquitocidal properties against mosquitoes of medical and veterinary importance (e.g., Amer and Mehlhorn 2006a, b, c, d; Benelli et al. 2015; Murugan et al. 2015a, b).

Furthermore, cancers figure among the leading causes of morbidity and mortality worldwide, with approximately 14 million new cases and 8.2 million cancer-related deaths in 2012. Among men, the five most common sites of cancer diagnosed in 2012 were lung, prostate, colorectum, stomach, and liver. Among women, the five most common diagnoses were breast, colorectum, lung, cervix, and stomach cancer. More than 60 % of world's total new annual cases occur in Africa, Asia, and Central and South America. These regions account for 70 % of the world's cancer deaths. It is expected that annual cancer cases will rise from 14 million in 2012 to 22 million within the next two decades (WHO 2015).

Nanotechnology is a promising field of interdisciplinary research, since it opens up a wide array of opportunities in different fields including pharmacology, electronics, parasitology, and pest management (Benelli 2016). Nanoparticles have received considerable attention in recent years due to their wide range of applications in the fields of diagnostics, biomarkers, cell labellings, antimicrobial agents, drug delivery, cancer therapy, and mosquito control (Elangovan et al. 2015; Benelli 2016). Titanium dioxide (TiO_2) nanoparticles have a wide array of commercial applications, particularly in consumer products such as various textiles, laundry additives, room sprays, water cleaners, and food storage containers. An emerging evidence suggests that the unique physical and chemical properties of TiO_2 nanoparticles, such as ultra-small size, increased surface area per unit mass, chemical composition, surface structure, shape, aggregation, and high reactivity, may pose potential risks to human health and the environment (Oberdorster et al. 2005; Marquis et al. 2009). Through inhalation, ingestion, and injection, TiO_2 nanoparticles can enter the human body, where they may interact with cells and components of cells, such as proteins and lipids, to compromise cellular functions, leading to cell toxicity (Yang et al. 2008). Thus, researchers are mainly focusing on the toxic effects of nanoparticles and also stressed that titanium and titanium alloys are one of the most used implant materials for biomedical applications, due to their outstanding properties, including high biocompatibility, resistance to body fluid effects, great tensile strength, flexibility, and high corrosion resistance (Kulkarni et al. 2015). TiO_2 is a photocatalyst, also widely utilized as a self-cleaning and self-disinfecting material for surface coating in many applications. Furthermore, it plays an helpful role in environmental purification, due to its nontoxicity, photo-induced super-hydrophobicity, and anti-fogging effect (Haghi et al. 2012). The small particle size of nanoparticles may allow different chemical, magnetic optical, and structural features, so they may have more differential toxicity profiles than normal-sized TiO_2. Consequently, TiO_2 nanoparticles have been recently classified as possible human carcinogen (group 2B) by the International Agency for Research on Cancer (IARC 2010). On the other hand, many toxicological studies were performed and several in vitro and in vivo toxicity tests have shown that metal nanoparticles do not penetrate human skin and cosmetic products containing metal nanoparticles were considered safe (Furukawa et al. 2011). However, in other studies, upon TiO_2 nanoparticle exposure, damage to lipids, proteins, and DNA leads to damage of subcellular organelles and cell death; the nanoparticles have been reported to induce chromatin condensation, nuclear fragmentation, caspase activation, and ultimately apoptosis (Park et al. 2008).

Several methods were employed for the synthesis of TiO_2 nanoparticles, ranging from chemical procedures, radiation, electrochemical, and photochemical methods. Recently, there have been a number of reports on the synthesis of TiO_2 nanoparticles of various shapes using the hydrothermal method. The hydrothermal synthesis of nanoparticles is more advantageous because it eliminates the elaborate process of maintaining microbial cultures and can also be suitably scaled up for large scale nanoparticles synthesis. Hydrothermal synthesis would have greater commercial viability if the nanoparticles could be synthesized more rapidly in the reaction vessels (Sohaebuddin et al. 2010; Thevenot et al. 2008). A common feature emerging from recent studies is that exposure of cells to TiO_2 nanoparticles increases the generation of reactive oxygen species (ROS) (Donaldson et al. 2003; Olmedo et al. 2005; Long et al. 2006, 2007). However, whether or not the increase of ROS is truly responsible for the cytotoxic effects of nanoparticles is still unknown.

In this research, we investigated the synthesis of TiO_2 nanoparticles using the hydrothermal method, and the nanoparticles were characterized by UV–Vis spectrophotometry, Fourier transform infrared spectroscopy (FTIR), X-ray diffraction (XRD), field emission scanning electron microscopy (FESEM), zeta potential, and energy-dispersive spectrometric analysis (EDX). The synthesized nanoparticles were tested for their larvicidal and pupicidal activity against the primary dengue vector *A. aegypti*. The antibacterial activity was evaluated against *Bacillus subtilis*, *Klebsiella pneumoniae*, and *Salmonella typhi* using the agar disk diffusion and minimum inhibitory concentration protocol. The impact of titanium dioxide nanoparticles on cell viability was studied assessing their in vitro cytotoxicity against human breast cancer cells (MCF-7) and normal breast epithelial cells (HBL-100). It has been elucidated that the synthesized TiO_2 nanoparticles had cytotoxic action against human breast cancer MCF-7 cells. The role of TiO_2 nanoparticles as a potent in vitro growth inhibitor of MCF-7 cells and its underlying mechanism of inhibition of TiO_2 nanoparticles were monitored through the induction of apoptosis.

Materials and methods

Synthesis and characterization of TiO_2 nanoparticles

Commercial titanium dioxide with a molecular weight of 79.88 and sodium hydroxide with a molecular weight of 40 were used (Sigma-Aldrich, Germany). Here, the mole ratio of TiO_2 is 1 M and the mass of the NaOH is calculated by taking 1 M. First, calculated mass of 1 g of NaOH is taken in the beaker containing 25 mL of distilled water. It was stirred for 30 min to obtain a clear solution. Then, calculated mass of 2 g TiO_2 is added to the abovementioned solution. The mixture was stirred vigorously and continuously for 24 h. The mixture was transferred to the alumina crucible and kept undisturbed for the setting of the sol–gel. Then, it was kept for drying at 50 °C. Finally, it was placed in a furnace at 400 °C for 2 h for the calcination of the sample. The sample was taken and made in very fine powder by grinding it in the mortar and pestle for 1 h, and TiO_2 nanopowder was obtained.

The sample was sonicated for uniform dispersion, and the optical properties of TiO_2 nanoparticles were monitored as a function of time in 10 mm optical path-length-quartz-cuvettes with Shimadzu, UV–Vis range 3600 spectrophotometer. Samples were diluted five times with distilled water before being measured. The morphology of the particles was examined by using FESEM (JSM 6390LV, JEOL, USA). Size distribution and the average size of the nanoparticles were estimated based on dynamic light scattering (DLS) with the assistance of Sigma-Scan Pro software (SPSS Inc., Version 4.01.003) and EDX spectrum. The grain size was determined by XRD analysis recorded by diffractometer (SEIFERT PTS 3003). Zetasizer (Malvern) instrumentation was used to analyze the surface charge of the particles. The functional groups present in the constituents on the reducing agent sodium hydroxide and their involvement in the synthesis of TiO_2 nanoparticles was determined by FTIR studies. The synthesized TiO_2 nanoparticles were mixed with KBr to make pellet, and the FTIR analysis was carried out by JASCO FT-IR 400. The particle size range of the nanoparticles along with its polydispersity was determined by using the particle size analyzer (Zetasizer, Malvern). Particle size was arrived based on measuring the time dependent fluctuation of scattering of laser light by the nanoparticles undergoing Brownian motion.

A. aegypti rearing

Pathogen-free laboratory-reared mosquitoes tested in this study were from a colony originally established as reported by Murugan et al. (2015b). Eggs of *A. aegypti* were provided by the National Centre for Disease Control (NCDC) field station of Mettupalayam (Tamil Nadu, India). Eggs were transferred to laboratory conditions (27±2 °C, 75–85 % RH, 14:10 (L/D) photoperiod) and placed in 18×13×4-cm plastic containers containing 500 mL of tap water, waiting for hatching. Larvae were fed daily with a mixture of dog biscuits and hydrolyzed yeast (3:1 ratio). Larvae and pupae were collected and transferred to plastic containers with 500 mL of water, until the testing phase (Murugan et al. 2015b).

Larvicidal toxicity

Following the methods reported by Murugan et al. (2015a, b). 25 *A. aegypti* larvae (I, II, III, or IV instar) or pupae were placed for 24 h in a 500-mL glass beaker filled with 250 mL of dechlorinated water plus the desired concentration of synthesized TiO_2 nanoparticles. Larval food (0.5 mg) was also provided. Each concentration was replicated five times against all instars. In control treatments, 25 larvae or pupae were transferred in 250 mL of dechlorinated water. Percentage mortality was calculated as follows:

$$\text{Percentage mortality} = (\text{number of dead individuals} / \text{number of treated individuals}) \times 100$$

Antibacterial activity

The bacteria tested in this study were purchased from Microbial Type Culture Collection and Gene Bank Institute of Microbial Technology Sector 39-A, Chandigarh, 160036 (India). Tested bacteria *were B. subtilis*, *K. pneumoniae*, and *S. typhi*. Eighteen- to 24-h-old bacterial cultures were used for preparation of the testing cultures. Nutrient broth composition was peptone (5 g/L), hydrolyzed yeast extract (1.50 g/L), beef extract (1.50 g/L), and sodium chloride (5 g/L). Final pH was

7.4. Following the method reported in Dinesh et al. (2015), 13 g of nutrient broth was suspended into 100 mL of distilled water (Dinesh et al. 2015). Twenty-five milliliters of the nutrient broth was transferred each into four conical glass flasks, and they were autoclaved at 121 °C for 15 min at 15 psi. After autoclaving the test tubes, each tested species was inoculated and incubated at 37 °C for 24 h. After 24 h, the culture attained 2×10^6 cfu/mL, which was further used for antibacterial assay. Antibacterial activity of titanium dioxide nanoparticles was assessed using the agar disk diffusion method (Clinical and Laboratory Standards Institute 2006). The tested bacteria were swabbed on the Muller Hinton agar medium plates. Three disks were inserted in each plate, treated with three different concentrations of the tested compounds. Then, plates were incubated at 37 °C for 24 h. After the incubation, the zones of inhibition (mm) were measured using a photomicroscope (Leica ES2, Germany) (Dinesh et al. 2015).

In vitro cytotoxicity of TiO_2 nanoparticles

MCF-7 and HBL 100 cells were purchased from the National Center for Cell Sciences (NCCS), Pune, and maintained in DMEM and McCoys 5a medium, supplemented with non-essential amino acids (Vivek et al. 2011). Cells were cultured at 37 °C in a humidified atmosphere containing 5 % CO_2 incubator. Cells were cultured as follows: $\sim1\times10^4$ cells/wells were seeded into 96-well tissue culture plates and incubated for 48 h. Both MCF-7 and HBL 100 cells were treated with series of 10–100 μg/mL concentrations of synthesized TiO_2 nanoparticles. The treated cells were incubated for 24 h for cytotoxicity analysis. The cells were then subjected 3-(4,5-dimethylthiazol-2-yl)-2,5-diphenyltetrazolium bromide (MTT) assay. The stock concentration (5 mg/mL) of MTT (a yellow tetrazole) was prepared, and 100 μL of MTT was added in each TiO_2 nanoparticle-treated wells and incubated for 4 h. Purple-colored formazone crystals were observed, and these crystals were dissolved with 100 μL of dimethyl sulphoxide (DMSO) and read at 620 nm in a multi-well ELISA plate reader (Thermo, Multiskan). OD value was subjected to sort out the percentage of viability by using the following formula (Vivek et al. 2012):

$$\text{Cell viability}\ (\%) = \frac{\text{Mean OD value of experimental sample } (TiO_2NP)}{\text{Mean OD value of experimental control (Untreated)}} \times 100$$

Morphological assays

The MCF-7 cells that were grown on coverslips (1×10^5 cells/cover slip) were incubated with TiO_2 nanoparticles with different concentration, and they were fixed in an ethanol/acetic acid solution (3:1, *v*/*v*). The coverslips were gently mounted on glass slides for morphometric analysis. Three monolayers per experimental group were photomicrographed. The morphological changes of the MCF-7 cells were analyzed using Nikon (Japan) bright field inverted light microscope at ×40 magnification.

Fluorescence microscopic analysis of apoptosis

Approximately 1 μL of a dye mixture (100 mg/mL acridine orange (AO) and 100 mg/mL ethidium bromide (EtBr) in distilled water) was mixed with 9 mL of cell suspension (1×10^5 cells/mL) on clean microscope coverslips. The cancer cells were collected, washed with phosphate-buffered saline (PBS) (pH 7.2), and stained with 1 mL of AO/EtBr. After incubation for 2 min, the cells were washed twice with PBS (5 min each) and visualized under a fluorescence microscope (Nikon Eclipse, Inc., Japan) at ×400 magnification with an excitation filter at 480 nm. The percentage of apoptotic cells was determined using the following formula:

$$\text{Apoptotic cells}\ (\%) = \frac{\text{Total number of apoptotic cells}}{\text{Total number of normal and apoptotic cells}} \times 100$$

4′,6-Diamidino-2-phenylindole dihydrochloride (DAPI) nuclear staining

MCF-7 cells were treated with the above methods for 48 h and then fixed with methanol/acetic acid (3:1, *v*/*v*) prior to washing with PBS. The washed cells were stained with 1 mg/mL DAPI for 20 min in the dark. Stained images were recorded with a fluorescent microscope with the appropriate excitation filter.

Western blot

Western blot was performed to detect the proteins of cytochrome c and β-actin. The MCF-7 cells (1×10^6) were seeded onto 100-mm culture dishes in the presence or absence of TiO_2 nanoparticles at inhibitory concentration (IC_{50}) concentrations for 24 h. Cells were washed twice with ice-cold PBS and incubated in lysis buffer. The lysates were centrifuged at 10,000×*g* for 5 min at 4 °C and were used as the cell protein extracts. Each of the extracts was applied to 12 % SDS polyacrylamide gel electrophoresis after which the proteins were transferred onto a nitrocellulose membrane and then blocked for 1 h using 10 % skim milk in water. After washing in PBS containing 0.1 % Tween 20 three times, the primary antibodies were added at a *v*/*v* ratio of 1:1,000. After overnight incubation at 4 °C, the primary antibodies were washed away and the secondary antibodies were added for 1-h incubation at room temperature. Finally, the

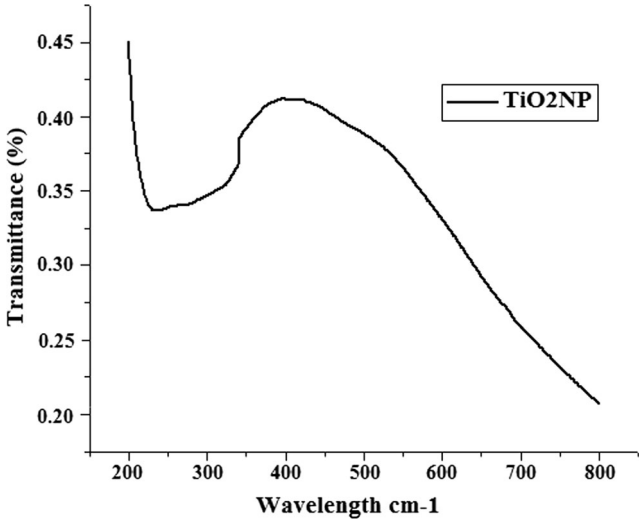

Fig. 1 UV–Vis spectrum of TiO_2 nanoparticles synthesized by hydrothermal method

enhanced chemiluminescence detection reagents were used to develop the signal of the membrane.

Data analysis

Mosquito mortality data were analyzed by probit analysis, calculating LC_{50} and LC_{90} following the method by Finney (1971). Bacteria inhibition growth data were transformed into arcsine/proportion values and then analyzed using a two-way ANOVA with two factors (i.e., the dosage and the bacterial species). Means were separated using Tukey's HSD test. $P<0.05$ was used for the significance of differences between means. All of the in vitro experiments were performed in triplicate. The statistical software SPSS version 17.0 was used. The P values were determined using the Student's t test, and a P value <0.05 was considered significant.

Results and discussion

Synthesis and characterization of TiO_2 nanoparticles

The chemical reduction of aqueous solution of titanium dioxide is one of the most widely used methods for the synthesis of TiO_2 nanoparticles in colloidal form. Under the UV region, TiO_2 nanoparticles give a characteristic absorbance band due to the excitation mode of their surface plasmons which is dependent on the nanoparticle size. These surface plasmon resonance (SPR) bands undergo towards a red shift or blue shift depending on the quantum size effects. The present study demonstrates the mechanism involved in the reduction of TiO_2 to TiO_2 nanoparticles by the chemical constituents of NaOH. The UV–Vis spectrum of TiO_2 nanoparticles synthesized using NaOH is reported in Fig. 1. The formation of TiO_2 nanoparticles was confirmed through the presence of an absorption peak at 380 nm. The production of TiO_2 nanoparticles was observed within 30 min when the NaOH was added to TiO_2 solution.

The FTIR spectrum of the synthesized TiO_2 nanoparticles (Fig. 2) showed strong absorption peak at 904 cm^{-1} indicating the presence of phenols (O-H group) and the presence of phenolic compound. Peaks close to 1,710 cm^{-1} indicated the presence of amine (N-H group) in the sample. It was assumed that phenolic compound in the NaOH solution might be involved in the reduction and formation of TiO_2 nanoparticles. The slight changes in the intensity at 2,142 cm^{-1} indicated the involvement of intermediate form of the phenolic group in the reduction process. On the other hand, the band shift at 910.37 cm^{-1} was attributed to the binding of the N-H functional group with titanium nanoparticles (see also Benelli 2016). The zeta potential measurement of TiO_2 nanoparticles showed the surface charges of the

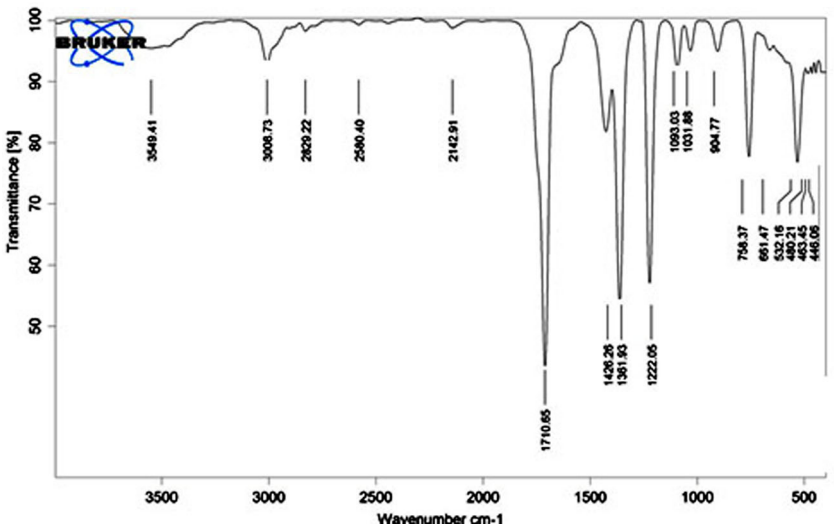

Fig. 2 FTIR spectrum of TiO_2 nanoparticles synthesized by hydrothermal method

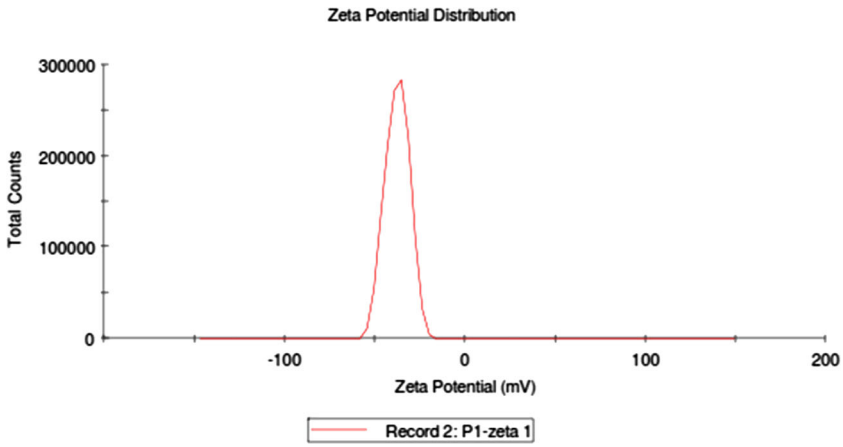

Fig. 3 Zeta potential analysis of TiO_2 nanoparticles synthesized by hydrothermal method

particles, with a value of −37.5 mV (Fig. 3), suggesting higher stability of synthesized TiO_2 nanoparticles. The large negative potential value could be due to the capping of polyphenolic constituents present in the reducing agent (see also Murugan et al. 2015b).

DLS analysis measured the shell thickness of a capping or stabilizing agent enveloping the metallic particles along with the actual size of the metallic core. The average size of the TiO_2 nanoparticles was also measured by DLS. The size distribution vs. intensity graph is reported in Fig. 4. The average size of TiO_2 nanoparticles was 70.80 nm. Larger particle sizes may also be due to the various forces of interaction in the solution like van der Waals forces. Different techniques give different size averages, depending on the instrument response to particle numbers, volume, mass, or optical property. Therefore, a great degree of caution needs to be taken when the particle sizes are measured by various techniques for a bio-based process and need to be compared to determine their reactivity for specific applications (Sujitha and Kannan 2013).

FESEM showed that TiO_2 nanoparticles were spherical in shape with size ranging from 20 to 100 nm (Fig. 5). The EDX profile of TiO_2 nanoparticles showed a strong peak of Ti (Fig. 6). The presence of O peaks along with the Ti signals, suggests that the TiO_2 nanoparticles were protected with phenolate ion. The XRD pattern of synthesized TiO_2 nanoparticles is showed in Fig. 7. The spectrum data revealed the occurrence of four major peaks that appeared with 2θ values, and these peaks correspond to the (111), (200), (220), and (311) planes of the face-centered cubic (fcc) phase, which are comparable with the standard (JCPDS 89-3722). The peak positions shed light on the translational proportion, namely the size and shape of the unit cell, while the peak intensities give details about the electron density inside the unit cell where the atoms are located. The width of the (111) peak was applied to calculate the average crystallite size using Scherrer equation.

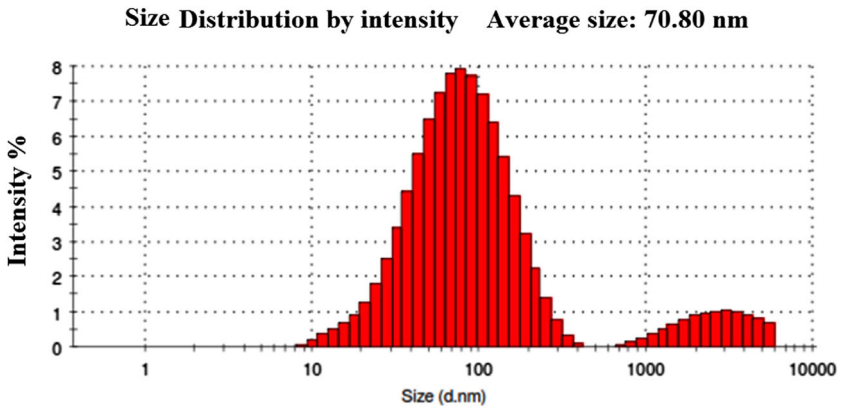

Fig. 4 DLS measurement to determine the size distribution of TiO_2 nanoparticles synthesized by hydrothermal method

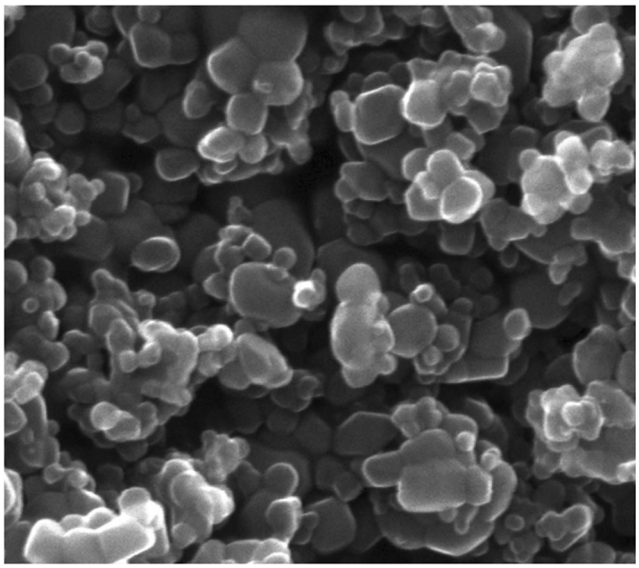

Fig. 5 SEM of TiO_2 nanoparticles synthesized by hydrothermal method

Larvicidal toxicity

Larvicidal and pupicidal experiments were conducted against the dengue mosquito *A. aegypti*. LC_{50} values of nanoparticles were 4.02 ppm (larva I), 4.962 ppm (larva II), 5.671 ppm (larva III), 6.485 ppm (larva IV), and 7.527 ppm (pupa) (Table 1). Recently, a growing number of eco-friendly routes have been proposed for the synthesis of nanoparticles toxic against young instars of several important mosquito vectors (see Benelli 2016 for a dedicated review). Concerning titanium ones, Rajakumar et al. (2014) showed that synthesized TiO_2 nanoparticles are highly toxic against lice, *Hyalomma anatolicum*, and the malaria vector *Anopheles subpictus*. Further studies also focused on the toxic activity of TiO_2 nanoparticles synthesized utilizing leaf aqueous extract of *Catharanthus roseus* against the adults of *Hippobosca maculata* and *Bovicola ovis*, with LD_{50} values of 7.09 and 6.56 mg/L, respectively (Velayutham et al. 2012).

Antibacterial activity

TiO_2-synthesized nanoparticles showed antibacterial properties against *B. subtilis*, *K. pneumoniae*, and *S. typhi*. At the maximum concentration tested (150 mg/L), titanium dioxide nanoparticles showed strong inhibitory action against *B. subtilis* (zone of inhibition 8.4 mm), *K. pneumoniae* (zone of inhibition 8.8 mm), and *S. typhi* (zone of inhibition 9.3 mm) (Table 2). Aqueous solution exposed to bacterial organisms changed in titanium hydrosol. The bacterial biomass was pale yellow before the addition of nanoparticles, then changed to light and dark brown (Table 3) (Dinesh et al. 2015). According to several studies, the metal oxides carry the positive charge while the microorganisms carry negative charges; we hypothesized that this causes electromagnetic attraction between microorganisms and the metal oxides which leads to oxidization and finally death of microorganisms (Zhang and Chen 2009). Overall, the bactericidal effect of the tested nanoparticles has been attributed to the decomposition of bacterial outer membranes by ROS, primarily hydroxyl radicals (OH), which leads to phospholipid peroxidation and ultimately cell death (Jayaseelan et al. 2013).

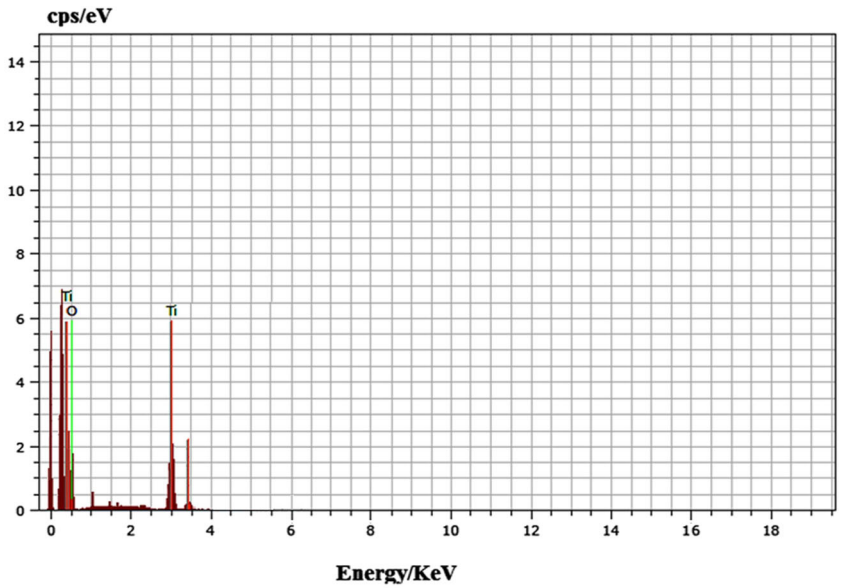

Fig. 6 EDX analysis of TiO_2 nanoparticles synthesized by hydrothermal method

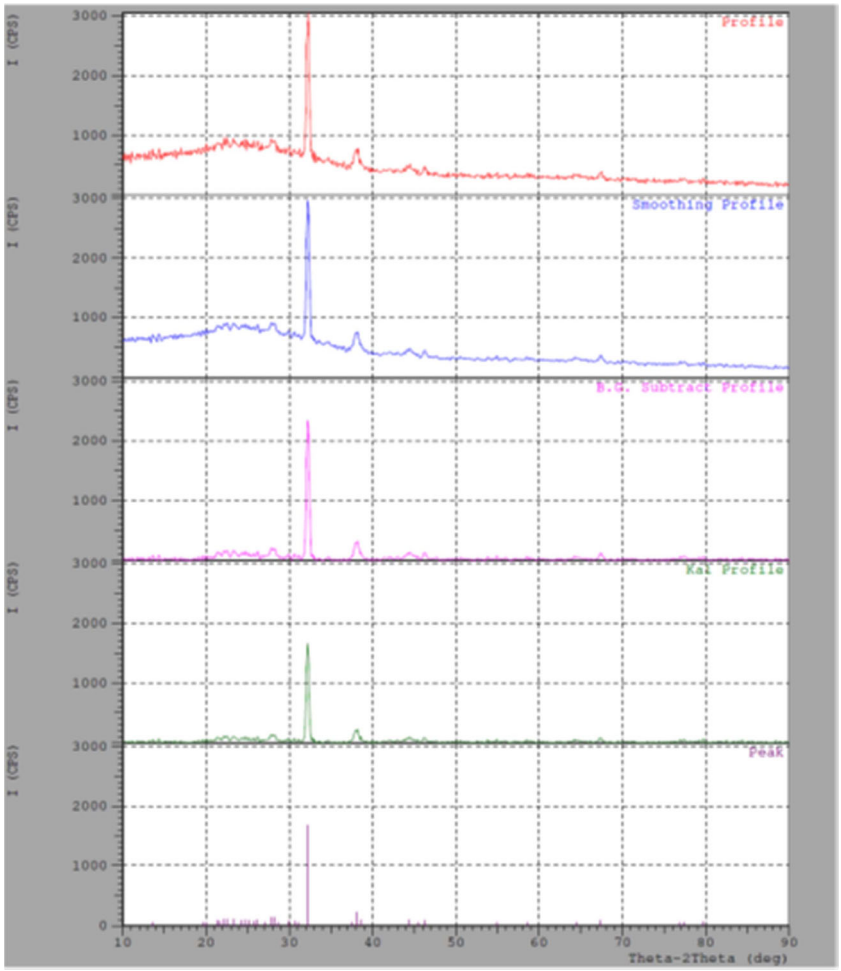

Fig. 7 XRD pattern of TiO_2 nanoparticles synthesized by hydrothermal method

Cell viability assays

TiO_2 nanoparticles as antibacterial agents are gaining greater demand in medical applications. At the same time, limited efforts have been conducted to shed light on the cytotoxic effects of synthesized TiO_2 nanoparticles, against cancer cell lines (Lagopati et al. 2010). Here, MTT assay was used to assess the effect of TiO_2 nanoparticles on proliferation of MCF-7 cells and HBL-100 cells. We investigated the induction of apoptosis as a possible mechanism for anti-proliferative activity of the synthesized TiO_2 nanoparticles. Dose-dependent cytotoxicity was observed in TiO_2 nanoparticle-treated MCF-7 cells. Fifty percentage of cell death (IC_{50}) of TiO_2 nanoparticles against MCF-7 cells was 60 μg/mL, while IC_{50} against HBL-100 cells was 80 μg/mL (Fig. 8). Similar reports about cell cytotoxicity of

Table 1 Larval and pupal toxicity effect of TiO_2 nanoparticles against filarial vector, *Aedes aegypti*

Target	LC_{50} (LC_{90})	95 % confidence limit LC_{50} (LC_{90})		Regression equation	χ^2 (*df*= 4)
		Lower	Upper		
Larva I	4.023 (8.482)	2.183 (7.002)	5.202 (11.951)	y=1.156+0.287x	8.047 n.s.
Larva II	4.962 (10.126)	3.460 (8.429)	6.140 (14.021)	y=1.232+0.248x	6.431 n.s.
Larva III	5.671 (11.411)	5.121 (10.381)	6.203 (12.888)	y=1.266+0.223x	1.431 n.s.
Larva IV	6.485 (13.088)	5.886 (11.713)	7.125 (15.177)	y=1.259+0.194x	0.637 n.s.
Pupa	7.527 (14.859)	6.848 (13.072)	8.366 (17.728)	y=1.316+0.175x	0.463 n.s.

No mortality was observed in the control

LC_{50} lethal concentration that kills 50 % of the exposed organisms, *LC_{90}* lethal concentration that kills 90 % of the exposed organisms, χ^2 chi-square value, *d.f.* degrees of freedom, *n.s.* not significant (α=0.05)

Table 2 Zone of inhibition of titanium nanoparticles against pathogenic bacteria

TiO_2 nanoparticles (mg/mL)	Inhibition zone (mm)		
	Bacillus subtilis	*Salmonella typhi*	*Klebsiella pneumoniae*
50	4.8±1.27 a	3.7±1.89 a	5.8±1.24 a
100	7.2±1.53 b	5.7±0.98 a	7.8±1.48 ab
150	8.4±1.12 b	8.8±1.54 b	9.3±1.65 b
Control	4.4±0.63 a	4.0±0.92 b	4.1±1.26 a

Values are means±SD of four replicates. Within each column, different letters indicate significant differences (Tukey's HSD test, $P<0.05$)

nanoparticles were discussed by Sukirtha et al. (2012) as well as by Murugan et al. (2016). While a number of in vitro studies indicated that the TiO_2 nanoparticles are toxic to the mammalian cells, our results also provide evidence of the higher cytotoxic effect of synthesized TiO_2 nanoparticles against breast cancer MCF-7 cell line compared with HBL-100 normal breast cell line.

Cancer cell death and nanoparticles-induced apopotosis

Morphological changes were observed in TiO_2 nanoparticle-treated MCF-7 cells when compared with untreated cells. The most recognizable morphological changes of TiO_2 nanoparticle-treated cells observed in this study were the cytoplasmic condensation, cell shrinkage, production of numerous cell surface protuberances at the plasma membrane, and the aggregation of the nuclear chromatin into dense masses beneath the nuclear membrane (Fig. 9).

The induction of apoptosis, after the treatment with IC_{50} concentration of TiO_2 nanoparticles, was assessed by fluorescence microscopy after staining with AO/EtBr. AO penetrated

Table 3 Color change of bacterial colonies from pale yellow to dark brown with 1 mM TiO_2

Time	Bacterium		
	Bacillus subtilis	*Salmonella typhi*	*Klebsiella pneumoniae*
0 min	−	−	−
10 min	−	−	−
30 min	−	−	−
1 h	−	+	−
2 h	+	++	+
4 h	++	++	++
8 h	++	++	++
16 h	+++	+++	+++
24 h	+++	+++	+++

− no color change, + slight color change, + pale yellow, ++ brownish, +++ dark brown

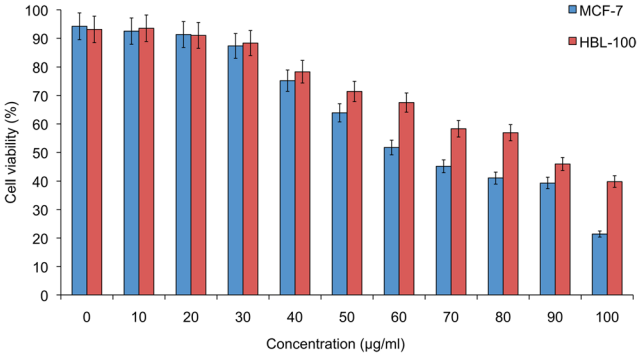

Fig. 8 MTT assays showing the in vitro cytotoxicity effect of TiO_2 nanoparticles against the MCF-7 cells and the normal HBL-100 cells after 24 h. IC_{50} concentrations were 60 and 80 µg/mL against MCF-7 and HBL-100, respectively. Data were expressed as mean±SD of three experiments. Cytotoxicity (%) is expressed relative to untreated controls (*$P<0.05$)

the normal cell membrane, and the cells were observed as green fluorescence. Apoptotic cells and apoptotic bodies were formed as a result of nuclear shrinkage and blebbing, and were observed as orange-colored bodies, whereas necrotic cells were observed as red color fluorescence due to their loss of membrane integrity when viewed under a fluorescence microscope (Fig. 9).

The TiO_2 nanoparticle-induced nuclear fragmentation was observed by DAPI staining. The untreated cells showed normal nuclei, whereas after treatment of MCF-7 cells with TiO_2 nanoparticles, the apoptotic nuclei (condensed or fragmented chromatin) were observed as shown in Fig. 9. Nuclear morphology analysis showed characteristic apoptotic changes, such as chromatin condensation, fragmentation of the nucleus, and formation of apoptotic bodies in the MCF-7 cells. In agreement with our findings, recent research pointed out that Ag nanoparticles can also induce DNA damage and apoptosis in cancer cells (Sanpui et al. 2011). In our experiments, by increasing the concentration of TiO_2 nanoparticles, the number of apoptotic cells increased, suggesting that TiO_2 nanoparticles induce cell apoptosis (Fig. 10).

Cell death via apoptosis is an important event in a number of immunological processes, as most of the anticancer drugs are believed to trigger apoptosis via mitochondria-mediated pathway (Shanthi et al. 2015). We here hypothesize that, as a new hybrid system, TiO_2 nanoparticles might also initiate the apoptosis via mitochondria-mediated pathway. This may be linked to the changes of the levels of mitochondrial-dependent apoptotic protein cytochrome c and β-actin. Consequently, we carried out Western blot to confirm cell apoptosis, analyzing the expression profiles of cytochrome c and β-actin. Western blot revealed the activation of

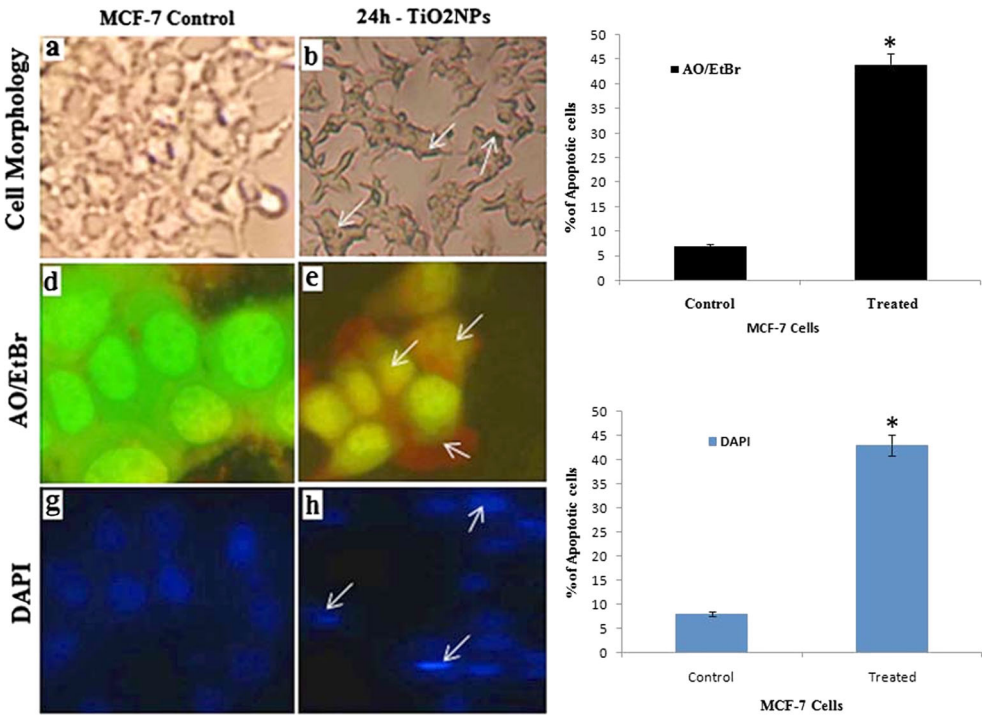

Fig. 9 Bright field and fluorescence microscopy of MCF-7 cells treated with IC_{50} concentrations of TiO_2 nanoparticles. Control cells and TiO_2 nanoparticle-treated cells observed using bright field microscope (**a** and **b**). Fluorescence microscopy of AO/EtBr-stained control cells and TiO_2 nanoparticle-treated cells (live cells in *green color*, in the treated sample indicated by *arrows*) (**c** and **d**). DAPI nuclear staining of control cells and TiO_2 nanoparticle-treated cells exhibited a condensed form of nuclear materials in apoptotic cells, which are indicated by *arrows* (**e** and **f**). Histogram representation of the percentage of total observed apoptotic cells against the IC_{50} concentration of TiO_2 nanoparticles formulated on selected MCF-7 cells after 24 h (*$P<0.05$)

cytochrome c expression profiles of these proteins in MCF-7 cells treated with TiO_2 nanoparticles. We observed that the expression of the cytochrome c proteins was significantly up-regulated in cells cultured with TiO_2 nanoparticles for 24 h (Fig. 10) when compared to untreated control β-actin. Similarly, it has been shown that the expression of both mRNA and protein level of cell cycle checkpoint gene p53 and pro-apoptotic gene (Bax and caspase-3) up-regulated and Bcl-2 down-regulated in HepG2 cell due to silica nanoparticle exposure (Gopinath et al. 2010).

Conclusions

Overall, this research highlights the effectiveness of TiO_2 nanoparticles acting as excellent mosquitocidal and antibacterial tools. Furthermore, the synthesized TiO_2 nanoparticles are able to exert cytotoxic effects on human breast cancer MCF-7 cells in vitro with lower toxicity on normal cells HBL-100. Further studies are required to elucidate the molecular mechanism involved in cell growth inhibition, thereby permitting the employment of synthesized TiO_2 nanoparticles as cancer chemopreventive and/or therapeutic agents.

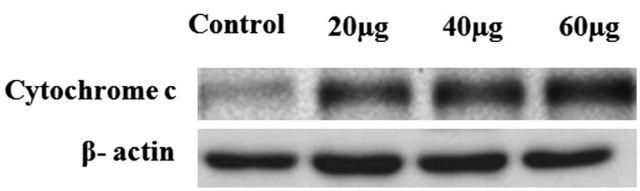

Fig. 10 Western blot analysis of cytochrome c and β-actin expression in breast cancer MCF-7 cells

Acknowledgments The authors would like to thank the financial support rendered by King Saud University, through the Vice Deanship of Research Chairs.

Compliance with ethical standards All applicable international and national guidelines for the care and use of animals were followed. All procedures performed in studies involving animals were in accordance with the ethical standards of the institution or practice at which the studies were conducted.

Conflict of interest The authors declare that they have no competing interests. G. Benelli is an Editorial Board Member of *Parasitology Research*. This does not alter the authors' adherence to all the *Parasitology Research* policies on sharing data and materials.

Informed consent Informed consent was obtained from all individual participants included in the study.

References

Amer A, Mehlhorn H (2006a) Larvicidal effects of various essential oils against *Aedes*, *Anopheles*, and *Culex* larvae (Diptera, Culicidae). Parasitol Res 99:466–472

Amer A, Mehlhorn H (2006b) Repellency effect of forty-one essential oils against *Aedes*, *Anopheles* and *Culex* mosquitoes. Parasitol Res 99:478–490

Amer A, Mehlhorn H (2006c) Persistency of larvicidal effects of plant oil extracts under different storage conditions. Parasitol Res 99:473–477

Amer A, Mehlhorn H (2006d) The sensilla of *Aedes* and *Anopheles* mosquitoes and their importance in repellency. Parasitol Res 99:491–499

Benelli G (2015) Research in mosquito control: current challenges for a brighter future. Parasitol Res 114:2801–2805

Benelli G (2016) Plant-mediated biosynthesis of nanoparticles as an emerging tool against mosquitoes of medical and veterinary importance: a review. Parasitol Res. doi:10.1007/s00436-015-4800-9

Benelli G, Murugan K, Panneerselvam C, Madhiyazhagan P, Conti B, Nicoletti M (2015) Old ingredients for a new recipe? Neem cake, a low-cost botanical by-product in the fight against mosquito-borne diseases. Parasitol Res 114:391–397

Clinical and Laboratory Standards Institute (2006) M7-A7 methods for dilution antimicrobial susceptibility tests for bacteria that grow aerobically; approved standard, 7th edn. Clinical and Laboratory Standards Institute, Wayne, PA

Dinesh D, Murugan K, Madhiyazhagan P, Panneerselvam C, Nicoletti M, Jiang W, Benelli G, Chandramohan B, Suresh U (2015) Mosquitocidal and antibacterial activity of green-synthesized silver nanoparticles from *Aloe vera* extracts: towards an effective tool against the malaria vector *Anopheles stephensi*? Parasitol Res 114:1519–1529

Donaldson K, Stone V, Borm PJ, Jimenez LA, Gilmour PS (2003) Oxidative stress and calcium signaling in the adverse effects of environmental particles (PM10). Free Radic Biol Med 34:1369–1382

Elangovan K, Elumalai D, Anupriya S, Shenbhagaraman R, Kaleena PK, Murugesan K (2015) Phyto mediated biogenic synthesis of silver nanoparticles using leaf extract of *Andrographis echioides* and its bio-efficacy on anticancer and antibacterial activities. J Photochem Photobiol B: Biol 151:118–124

Finney DJ (1971) Probit analysis. Cambridge University Press, London

Furukawa F, Doi Y, Suguro M, Morita O, Kuwahara H, Masunaga T (2011) Lake of skin carcinogenicity of topically applied titanium dioxide nanoparticles in the mouse. Food Chem Toxicol 49:744–749

Gopinath P, Gogoi SK, Sunpui P, Pual A, Chattupadhyay A, Ghosh SS (2010) Signaling gene cascade in silver nanoparticle induced apoptosis. Colloids Surf B 77:240–245

Haghi M, Hekmatafshar M, Janipour MB, Gholizadeh SS, Faraz MK, Sayyadifar F, Ghaedi M (2012) Antibacterial effect of TiO_2 nanoparticles on pathogenic strain of *E. coli*. Int J Adv Biotechnol Res 3:621–662

IARC (2010) Monographs on the evaluation on carcinogenics risks to humans, vol 93. Carbon block, Titanium dioxide and Talc, Lyon, France

Jayaseelan C, Rahuman AA, Roopan SM, Kirthi AV, Venkatesan J, Kim S, Iyappan M, Siva C (2013) Biological approach to synthesize TiO2 nanoparticles using *Aeromonas hydrophila* and its antibacterial activity. Spectrochim Acta Part A: Mol Biomol Spectrosc 107: 82–89

Kovendan K, Murugan K, Shanthakumar SP, Vincent S, Hwang JS (2012) Larvicidal activity of *Morinda citrifolia* L. (Noni) (Family: Rubiaceae) leaf extract against *Anopheles stephensi*, *Culex quinquefasciatus*, and *Aedes aegypti*. Parasitol Res 111:1481–1490

Kulkarni M, Mazare A, Gongadze E, Perutkova S, Kralj-Iglic V, Milosev I, Schmuki P, Iglic A and Mozetic M (2015) Titanium nanostructures for biomedical applications. IOB Publishing. Nanotechnology 26. doi: 10.1088/0957-4484/26/6/062002

Lagopati N, Kitsiou PV, Kontos AI, Venieratos P, Kotsopoulou E, Kontos AG, Dionysiou DD, Pispas S, Tsilibary EC, Falaras P (2010) Photo-induced treatment of breast epithelial cancer cells using nanostructured titanium dioxide solution. J Photoch Photobiol A 214:215–223

Long TC, Saleh N, Tilton RD, Lowry GV, Veronesi B (2006) Titanium dioxide (P25) produces reactive oxygen species in immortalized brain microglia (BV2): implications for nanoparticle neurotoxicity. Environ Sci Technol 40:4346–4352

Long TC, Tajuba J, Sama P, Saleh N, Swartz C et al (2007) Nanosize titanium dioxide stimulates reactive oxygen species in brain microglia and damages neurons in vitro. Environ Health Perspect 115: 1631–1637

Marquis BJ, Love SA, Braun KL, Haynes CL (2009) Analytical methods to assess nanoparticle toxicity. Analyst 134:425–439

Murugan K, Benelli G, Ayyappan S, Dinesh D, Panneerselvam C, Nicoletti M, Hwang JS, Mahesh Kumar P, Subramaniam J, Suresh U (2015a) Toxicity of seaweed-synthesized silver nanoparticles against the filariasis vector *Culex quinquefasciatus* and its impact on predation efficiency of the cyclopoid crustacean *Mesocyclops longisetus*. Parasitol Res 114:2243–2253

Murugan K, Benelli G, Panneerselvam C, Subramaniam J, Jeyalalitha T, Dinesh D, Nicoletti M, Hwang JS, Suresh U, Madhiyazhagan P (2015b) *Cymbopogon citratus*-synthesized gold nanoparticles boost the predation efficiency of copepod *Mesocyclops aspericornis* against malaria and dengue mosquitoes. Exp Parasitol 153:129–138

Murugan K, Aruna P, Panneerselvam C, Madhiyazhagan P, Paulpandi M, Subramaniam J, Rajaganesh R, Wei H, Saleh Alsalhi M, Devanesan S, Nicoletti M, Syuhei B, Canale A, Benelli G (2016) Fighting arboviral diseases: low toxicity on mammalian cells, dengue growth inhibition (in vitro) and mosquitocidal activity of *Centroceras clavulatum*-synthesized silver nanoparticles. Parasitol Res. doi:10.1007/s00436-015-4783-6

Oberdorster G, Oberdorster E, Oberdorster J (2005) Nanotoxicology: an emerging discipline evolving from studies of ultrafine particles. Environ Health Perspect 113:823–839

Olmedo DG, Tasat DR, Guglielmotti MB, Cabrini RL (2005) Effect of titanium dioxide on the oxidative metabolism of alveolar macrophages: an experimental study in rats. J Biomed Mater Res A 73: 142–149

Park EJ, Yi J, Chung KH, Ryu DY, Choi J (2008) Oxidative stress and apoptosis induced by titanium dioxide nanoparticles in cultured BEAS-2B cells. Toxicol Lett 180:222–229

Rajakumar G, Abdul Rahuman A, Jayaseelan C, Santhoshkumar T, Marimuthu S, Kamaraj C, Bagavan A, Abduz Zahir A, Vishnu Kirthi A, Elango G, Arora P, Karthikeyan R, Manikandan S, Jose S (2014) Solanum trilobatum extract-mediated synthesis of titanium dioxide nanoparticles to control Pediculus *humanus capitis*, *Hyalomma anatolicum anatolicum* and *Anopheles subpictus*. Parasitol Res 113:469–479

Sanpui P, Chattopadhyay A, Ghosh SS (2011) Induction of apoptosis in cancer cells at low silver nanoparticle concentrations using chitosan nanocarrier. ACS Appl Mater Interf 3:218–228

Shanthi K, Vimala K, Gopi D, Kannan S (2015) Fabrication of pH responsive DOX conjugated PEGylated palladium nanoparticle mediated drug delivery system: an in vitro and in vivo evaluation. RSC Adv 5:44998–45014

Sohaebuddin SK, Thevenot PT, Baker D, Eaton JW, Tang L (2010) Nanomaterial cytotoxicity is composition, size, and cell type dependent. Part Fibre Toxicol 7:22

Sujitha MV, Kannan S (2013) Green synthesis of gold nanoparticles using Citrus fruits (*Citrus limon*, *Citrus reticulata* and *Citrus sinensis*) aqueous extract and its characterization. Spectrochim Acta Part A: Mol Biomol Spectrosc 102:15–23

Sukirtha R, Priyanka K, Antony JJ, Kamalakkannan S, Thangam R, Gunasekaran P (2012) Cytotoxic effect of green synthesized silver nanoparticles using *Melia azedarach* against in vitro HeLa cell lines and lymphoma mice model. Process Biochem 47:273–9

Thevenot P, Cho J, Wavhal D, Timmons RB, Tang L (2008) Surface chemistry influences cancer killing effect of TiO_2 nanoparticles. Nanomedicine 4:226–236

Velayutham K, Rahuman AA, Rajakumar G, Santhoshkumar T, Marimuthu S, Jayaseelan C, Bagavan A, Kirthi AV, Kamaraj C, Zahir AA, Elango G (2012) Evaluation of *Catharanthus roseus* leaf extract-mediated biosynthesis of titanium dioxide nanoparticles against *Hippobosca maculata* and *Bovicola ovis*. Parasitol Res 111:2329–2337

Vivek R, Kannan S, Achiraman S, Thirumurugan R, Ganesh DS, Krishnan M (2011) Survivin deficiency leads to imparalization of cytokinesis in cancer cells. Asian Pac J Cancer Prev 12:1675–9

Vivek R, Thangam R, Muthuchelian K, Gunasekaran P, Kavery K, Kannan S (2012) Green biosynthesis of silver nanoparticles from *Annona squamosa* leaf extract and its in vitro cytotoxicity effect on MCF-7 cells. Process Biochem 47:2405–2410

WHO (2012). Dengue and severe dengue: fact sheet no. 117 [webpage on the Internet] Geneva: [cited March 4, 2013]. http://www.who.int/mediacentre/factsheets/fs117/en/index.html

WHO (2015) Cancer. Factsheet N. 297, Geneva

Yang W, Peters JI, Williams RO III (2008) Inhaled nanoparticles—a current review. Int J Pharm 356:239–247

Zhang H, Chen G (2009) Potent antibacterial activities of Ag/Tio2 nanocomposite powders synthesized by a one-potsol-gel method. Environ Sci Technol 934(8):2905–2910